100-year waves, teleconnections and wave climate variability

P.H. TAYLOR*, V.E. BARKER, D. BISHOP, R. EATOCK TAYLOR

Department of Engineering Science, University of Oxford,
Parks Road, Oxford, U.K.

*paul.taylor@eng.ox.ac.uk

11th International Workshop on Wave Hindcasting and Forecasting, Halifax, Canada

1. Introduction

The design of any offshore structure is governed to a great extent by the severity of the environment, so specification of the extremes of the wave field remains a key issue. Does it make sense to talk about the average wave climate at a particular location? Are the properties of waves over the last 25 years a reliable guide to what may happen in the next 25 or 100 years? These questions are tackled by seeking correlations between a varying 100-year wave estimate based on a 5-year sliding window over the available wave data and much larger-scale geophysical variations, the so-called 'teleconnections', such as the North Atlantic Oscillation for offshore Norway and the Pacific/North American pattern for the north Pacific. The approach works well, particularly for offshore Norway because the correlation to the NAO is high and NAO data is available back to 1828, allowing the variation of the extreme wave climate over almost 200 years to be examined. In contrast, at two of the four points we have looked at in the north Pacific, the wave climate is severe but remarkably constant – these points being close to a node of the PNA pattern. Elsewhere in the north Pacific the variation over time is much larger, and both the PNA index and the NAO are significantly correlated to the varying wave climate.

Predicting extreme wave characteristics is difficult with problems arising in both the statistics and geophysics. Measured wave records from instrumented buoys are rarely over 35 years long and often contain gaps, meaning that observed extreme values are scarce and so the wave characteristics derived are uncertain (Menendez, 2008). Large-scale geophysical variation across the oceans also present problems as buoys are few and irregularly spaced so assessing spatial variation is difficult. Furthermore, climate variation may have timescales of 50 years or more so assessing correlations in the timeframe of a buoy record is inherently unreliable.

Recurring and persistent, large-scale patterns of pressure and circulation anomalies that span vast geographical areas are known as teleconnections. In engineering terms teleconnections represent the modes of low frequency climate variability of the coupled atmosphere-ocean system. The relationship between extreme waves and the climate is an interesting and important one but as yet not well understood. There is much information that climatologists, geophysicists and engineers can gain from exploring such relationships.

Firstly, climate indices are available for much longer periods than wave records (the NAO is tabulated from 1823) and so, using empirical relationships, it might be possible to infer the wave history at any location over a much longer period than that for which directly measured data is available. Secondly, the empirical relationships provide a means of forecasting long and short-term future wave climates. Thirdly, society's increased awareness of the effects of climate change have led to inevitable postulates of a link between extreme waves and global warming. In the late 20th century studies found a trend of increasing wave heights in the Atlantic (Carter and Draper, 1988: Bacon and Carter, 1991) and later in the Pacific (Allan and Komar, 2000).

The most used design wave in this paper is the 'one hundred year wave'. When engineers discuss the one hundred year wave, they are acknowledging that, in a given year, there is a risk of 10^{-2} that the design wave will be exceeded.

2. Methodology

2.1 North Pacific Data

Data from the North Pacific is collected from moored buoys operated by NDBC (National Data Buoy Centre). The study used 4 stations in the North Pacific, shown in Figure 1. The requirements for station selection were as follows: a long and complete wave record, away from shallow water and coastal effects, geographical spread, location away from the tropics and large waves.

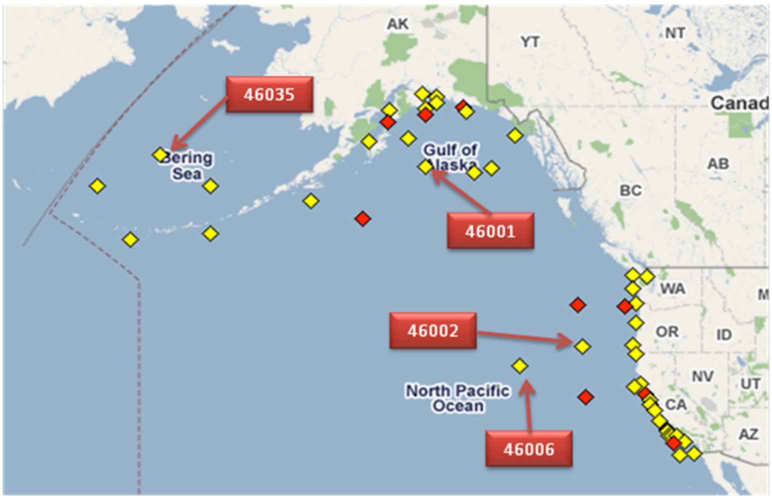

Figure 1. Locations of buoys chosen for this study (Google Maps and NDBC)

2.2 Norwegian data

This data is a mixture of data measured at an oceanographic buoy in the Haltenbanken area west of Trondheim, Norway, and also hindcast results used to fill in gaps in the measured data, taken from the Skarv and Heidrun fields. The location is shown in Figure 2.This merged dataset was provided by BP.

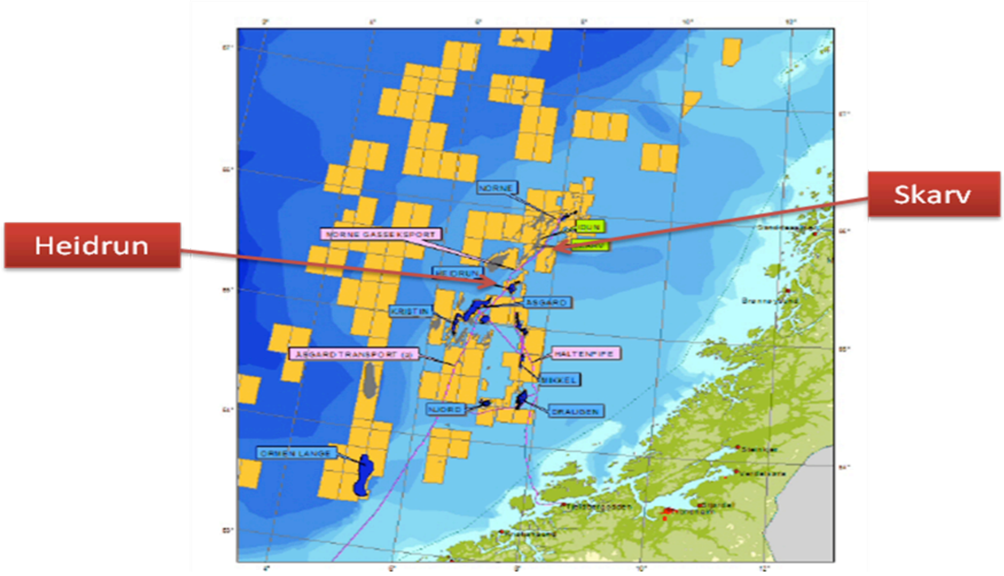

Figure 2. Location of the Haltenbanken area west of Norway (www.bp.com)

2.3 Storm identification

Most simple extrapolation techniques require that successive data observations should be identically distributed and uncorrelated. However, successive Hs values are strongly correlated, Hs being the average 4x the standard deviation of the free-surface displacement as waves pass by. A method developed by Tromans and Vanderschuren (1995) is to split the Hs record into storms, which are effectively uncorrelated. The datasets used in this work give Hs values hourly. The maximum hourly-averaged Hs value in any storm is termed ‘Hs-max’ and may be used as one of the characteristic parameters for any storm.

Hmp is the most probable maximum individual wave height in a storm. The use of the statistically robust parameter Hmp reflects the possibility that the largest wave in a storm may not occur in the most severe hourly interval for the storm and that storms typically last considerably longer than 1 hour (Tromans and Vanderschuren (1995), Taylor and Goh (2000)). For each storm the following methodology is used. Assume a Rayleigh distribution for individual wave heights in each hourly H_s interval. The wave period (T_z) gives N, number of waves per hour. Select a value for A (amplitude = wave height H/2) for the largest individual wave in each hour of assumed constant Hs value in the storm by random sampling from the Rayleigh Distribution. The probability (P) that all N peaks are simultaneously less than A is:

$$P = \left[1 - \exp\left(-\frac{A^2}{2\sigma^2}\right)\right]^N \quad \textbf{Equation 1} \qquad \text{with} \qquad \sigma = \frac{H_s}{4}$$

The probability P is chosen to be a random number between 0 and 1, hence a value for A can be deduced.

This is repeated for each hour in the storm and the maximum estimated A value (A_{max}) at any time during the storm is found. The whole process is repeated 1000 times enabling a histogram to be constructed to which an empirical pdf can be fitted:

$$p = \frac{dP}{dA} = \frac{AN}{\sigma^2}\exp\left(-\frac{A^2}{2\sigma^2}\right)\left[1 - \exp\left(-\frac{A^2}{2\sigma^2}\right)\right]^{N-1} \qquad \textbf{Equation 2}$$

The fit is done by doing a two parameter optimization for the variables σ and N. The objective is to minimise the error between the empirical pdf and the normalized histogram in a least squares sense. Amp is the peak value of the fitted pdf. Therefore the peak of the distribution is found by differentiation of Equation 3 with respect to A. Then, the most probable extreme wave height within this storm is Hmp = 2x Amp for linear wave theory. The process is illustrated in Figure 3. Although we make no further use of the values, it is interesting to note the fitted σ and N, these are the standard deviation and number of waves in an equivalent rectangular storm with the same statistical distribution for the extreme wave height as the real storm.

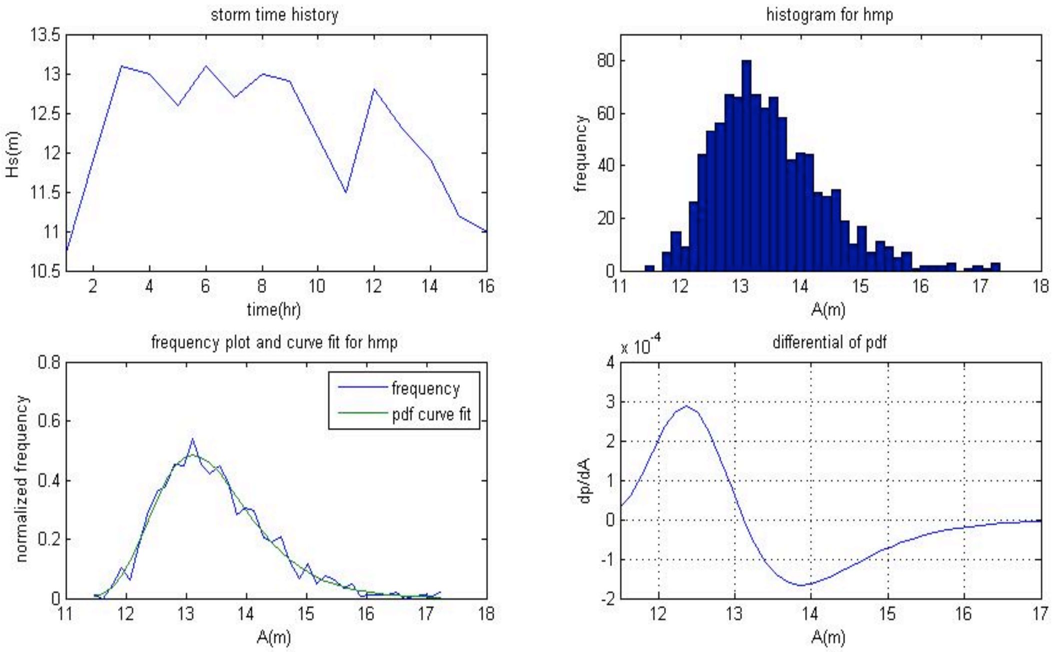

Figure 3. An example of calculating Hmp for the storm of 15/12/87 as recorded by buoy 46035 (Bering Straits).

From top left: the time history of Hs, a histogram of the sampled A values, a frequency plot with the empirical pdf shown in green and the differential of the pdf is given with the zero crossing on the vertical axis at Amp=Hmp/2.

2.4 POT analysis

Having identified each storm and a measure of the severity, the storms are ordered in terms of severity of Hmp. After ranking the storms at each station, a plot of the logarithm of that rank against Hmp, an exceedance plot, is produced. To gauge the variability in the estimates of the storm statistics, the data was bootstrapped. The underlying assumption of the bootstrap is that the best fit for the data is the data itself. Bootstrapping is a computational technique developed by Efron at Stanford (Diaconis and Efron 1983). It involves random sampling with replacement from the dataset to produce synthetic datasets which vary from the original only by sample variability – this is useful for assessing the effects of the finite size of the dataset on the resulting statistical fits.

Following the Peaks over Threshold (POT) methodology the objective is to find a form of cumulative density function (cdf) tail that fits to the exceedance graphs yielding extrapolation to the long term storm statistics. Two fitting forms were considered, w2 and cw3, both variants of the Weibull distribution:

$$\log_{10} N = a + b\, Hmp^{c}$$ **Equation 3 The 2 parameter Weibull fit (w2)**

$$\log_{10} N = a + b\, Hmp + c\, Hmp^{2}$$ **Equation 4 The constrained Weibull 3 model (cw3)**

Bootstrapping was used to estimate confidence intervals within which 90% of the storm statistic estimates lie. On the plots this has the form of an envelope, or trumpet.

In order to provide insight into how storm statistics vary over time, the concept of a sliding window plot is introduced. This is based on blocks of data from five successive winters, denoted in terms of the year by 1st

Jan of the central year and the two years either side of it. Other than reducing the number of storms considered for each fit, the five-year based Hmp-100 values are estimated in exactly the same manner as the conventional Hmp-100 for the entire record.

North Pacific results

Statistic	Model	Station 46001	46002	46006	46035
Hmp-100 (m)	**w2**	26.67	28.25	32.38	31.92
	cw3	26.70	28.15	31.80	31.91
Hmp-1000 (m)	**w2**	29.94	32.22	38.44	37.32
	cw3	29.97	32.00	37.28	37.27

Table 1. North Pacific results: prediction of the hundred year (Hmp-100) and thousand year (Hmp-1000) conditions based on bootstrap means.

The more extreme wave climates of stations 46035 and 46006 compared to 46001 and 46002 are clear in Table 1. The difference is so large that the hundred year conditions at 46006 and 46035 are comparable with those at the thousand year level at 46001 and 46002.

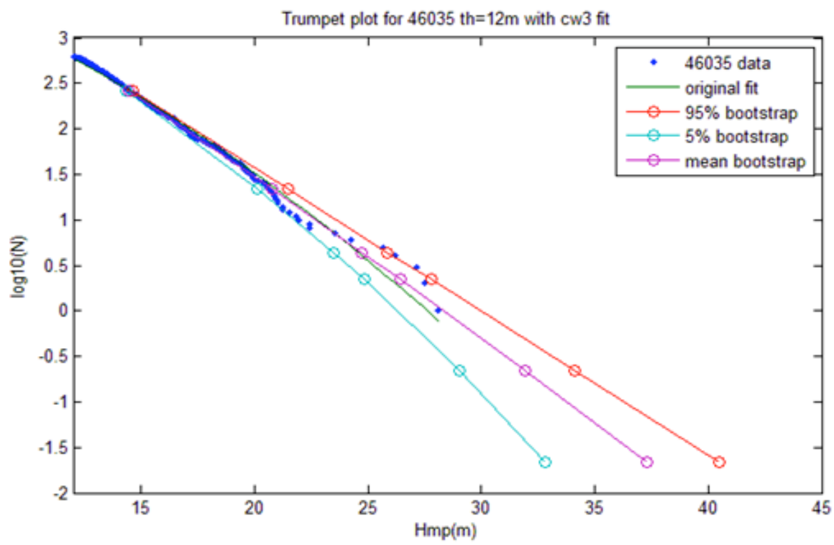

Figure 4. Trumpet plot for 46035 (Bering Sea) with a 12m threshold and constrained Weibull cw3 fit for the whole record. The lowest row of circles correspond to a return period of 1000 years, the 2nd lowest of 100 years etc.

A typical example of the exceedance or trumpet plot is shown in Figure 4. Every data point (in blue) corresponds to an individual measured storm, and these all lie within or very close to the trumpet. The bottom lowest circles on each fit curve correspond to return periods of 10,100 and 1000 years. Generally, the variation of the 5-95% hundred year condition (Hmp-100) is 5-6m, which is approximately 15% of the estimated value. This level of uncertainty would be reasonable to work with when designing an offshore facility, and is essentially unavoidable given the short duration of the original dataset. One important result is that, for all the cases studied, the choice of the model fitted (w2 or cw3) makes only a very slight difference in the storm statistics.

Figure 5 shows the prediction of the variation of the 100-year Hmp based on a sliding window of 5-years worth of data, the definition of the storm year being based on the year for 1st January of the third winter, and two winters either side. The only differences between these 5-year sliding window predictions and the original fits to the entire datasets are the number of storms included and the choice of the threshold for the POT-analysis, the 5-year sliding windows estimates using a 10m threshold rather than the 12m used when analysing the entire dataset at once. Also shown in Figure 5 are the 5-95% confidence bands based on simple bootstrapping.

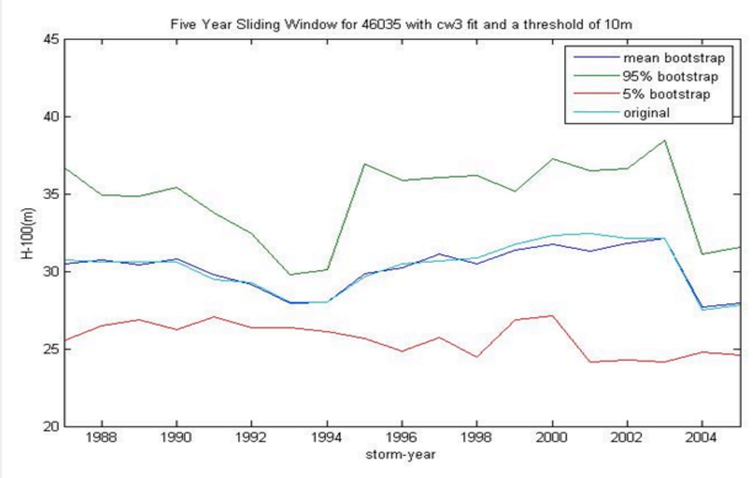

Figure 5. Five Year Sliding Window for 46035 with cw3 fit and threshold of 10m. The mean of the bootstraps and the fit to the original data are remarkably similar. This is true for all thresholds and both fitting models for all stations.

Figure 6 shows 100-year predictions on the basis of a 5-year sliding window of storm severity for all the Pacific stations. The top part shows the 100-year estimates from the fits to the buoy data. The lower part shows the variation of the mean of the bootstrapped estimates. For all four Pacific stations the simple fitted values and the mean of the bootstraps match very well, showing very similar variation over time. It is interesting that the two locations with less severe wave climate show noticeably smaller variation over time than the two more severe locations.

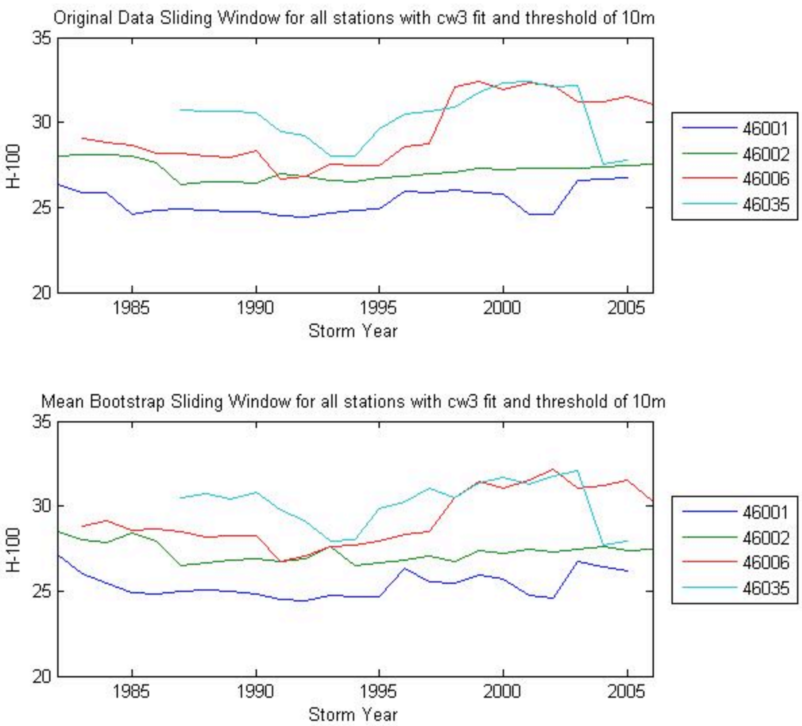

Figure 6. Sliding window fits to 100-year extreme wave for all stations with a threshold of 10m and cw3 fit. Locations 46001 and 46002 exhibit particularly low variation of Hmp-100. Top – fit to original data. Bottom – mean fit to bootstrapped datasets.

North Atlantic results

Exactly the same methodology was used to analyse the Norwegian data as was used for the North Pacific. Figure 7 shows the exceedance plot, again showing the precise form of the Weibull fit is unimportant.

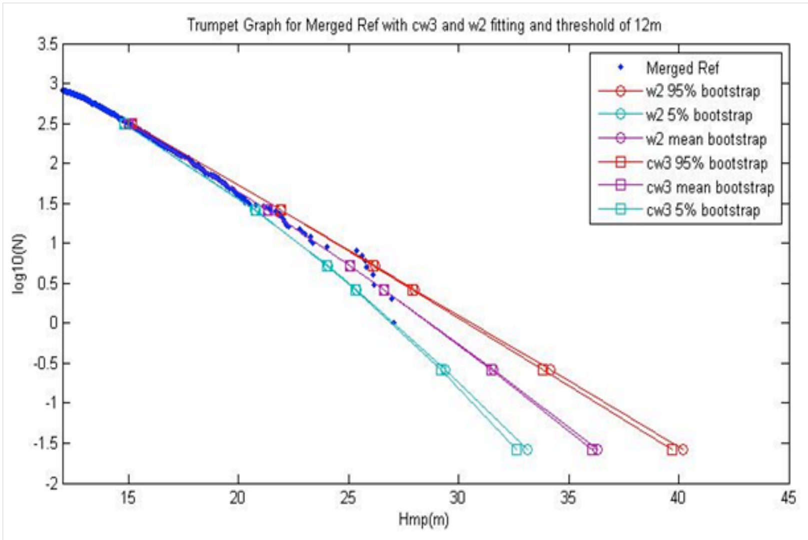

Figure 7. Trumpet Plot for Haltenbanken with cw3 and w2 fitting and threshold of Hmp=12m, showing similar results to the Pacific stations.

3. Extreme waves and teleconnections

The North Atlantic Oscillation (NAO) is a predominantly atmospheric mode measured by the normalized sea level pressure difference between Gibraltar and South-West Iceland (the centres of action). The positive phase of the NAO reflects below normal pressure across the high latitudes of the North Atlantic and above normal pressure over the central North Atlantic, the eastern United States and Western Europe. The negative phase reflects an opposite pattern of pressure anomalies over these regions. The wintertime NAO exhibits significant multi-decadal variability (Hurrell et al., 2003). Storm tracks vary from one year to the next but the NAO gives an indication of the magnitude of these storms and in particular their north-south movement (Osborn, 2006).

The NAO in a high positive state can be thought of causing strong and persistent westerlies that drive large storms towards Northern Europe. Large negative values cause the tracks of the westerlies to move further south, so fewer and less severe storms reach northern Europe.
So is the NAO visible in the 5-year sliding window predictions of the 100-year extreme wave?

Figure 8 shows variation of the 100-year Hmp values using a 5-year sliding window for the Haltenbanken buoy dataset and the winter values of the NAO index averaged over the same sliding window. There is a strong similarity between the two functions, with a correlation R^2 coefficient of 0.83, so we conclude *there is a significant link between the NAO and the 5-year based estimates of the 100-year wave offshore mid-Norway*.

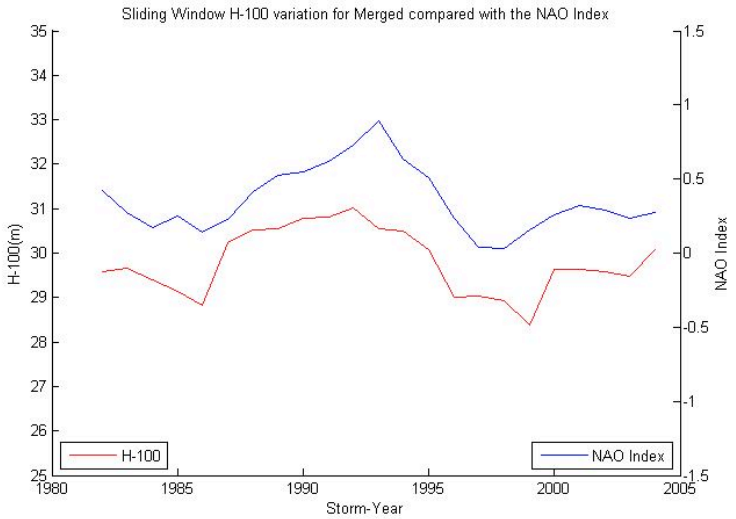

Figure 8. Sliding Window of Haltenbanken Hmp-100 prediction and the winter averaged NAO index

The correlation is consistent with the work of Woolf et al. (2002) based on the relationship between satellite measured wave heights and the NAO, albeit they worked with the averaged wave climate rather than estimates for the 100-year extremes of the wave field.

3.1 An NAO-based wave predictor for offshore Norway

The pressure-based NAO index is available back to the 1820s (data from Osborn: www.cru.uea.ac.uk). Thus, the exciting possibility arises of back-predicting extreme wave severity over almost the last 200 years. The NAO index is plotted against the H-100 prediction parametrically over the period 1982-2004. A least-squares linear fit between the two variables is applied with 5-95% confidence limits (Figure 9).

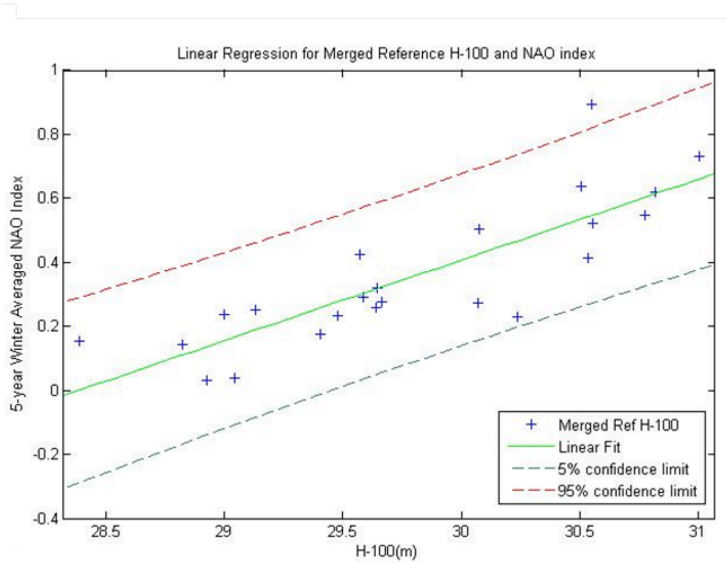

Figure 9. Linear fit for Haltenbanken 100-year Hmp wave height with the NAO index.

This yields an estimator for the 100-year Hmp (m) at Haltenbanken based on the NAO index of

$$H_{mp-100} = 4\,NAO + 28.6 \quad \textbf{Equation 6}$$

Using the linear relationship as a predictor, it is then possible to back-infer the wave climate based on the NAO-index with good accuracy, as shown in Figure 10.

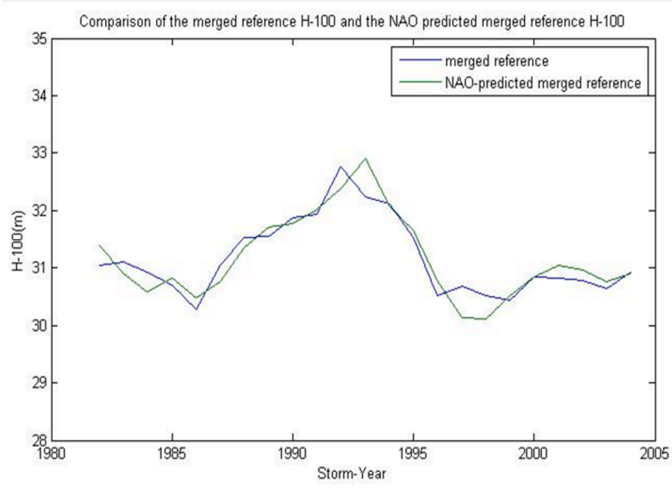

Figure 10. Comparison of Hmp-100 derived from the buoy data and from the NAO-based predictor for Haltenbanken.

Figure 11 shows the estimated extreme 100-year wave off Norway over the entire period for which pressure-based NAO data is available, showing very large variations in the wave climate. One interesting observation for the NAO-based prediction is that at times over the last 200 years the wave climate has been significantly worse than any observations of waves since 1960 would suggest - an important possibility given that all new observations of extremes are immediately attributed to climate change by the world's press.

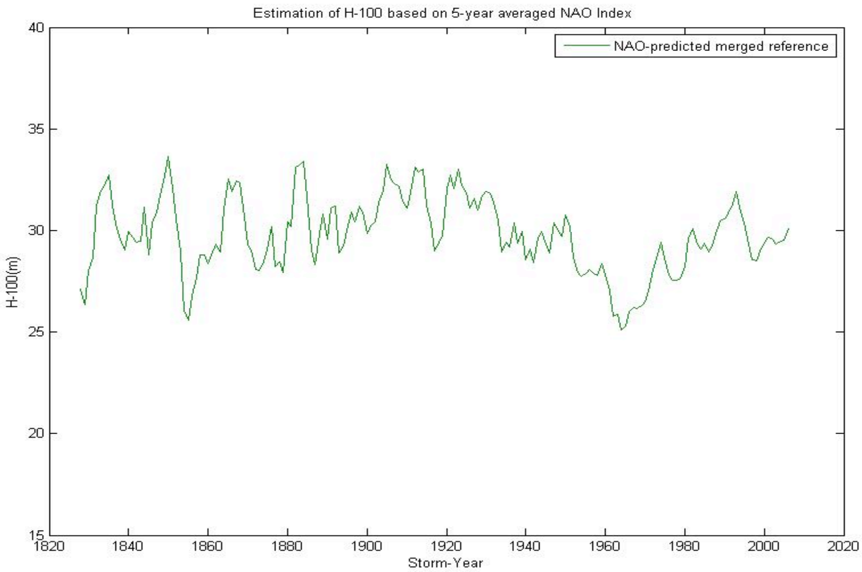

Figure 11. Estimation of 5-year sliding window based Hmp-100 over 200 years at Haltenbanken offshore Norway based on 5-year averaged NAO Index.

3.2 Extreme Waves and Climate Indices for the north Pacific

Five Pacific Ocean related climatic phenomena were considered: East-Pacific/North-Pacific (EP/NP), Pacific/North American (PNA), El Nino/Southern Oscillation (ENSO), and Pacific Decadal Oscillation (PDO), together with the North Atlantic Oscillation (NAO). The nature of each Pacific index is briefly described in the Appendix.

The correlation coefficients between the 5-year sliding window Hmp-100 wave heights and the various climate indices are given in Table 3. Recall that the wave climates for stations 46001 (Gulf of Alaska) and

46002 (inshore California/Oregon) are remarkably constant, so the correlations for these describe very small changes. In contrast, stations 46006 (offshore California) and 46035 (Bering Sea) both show significant changes in their wave climates, as shown in Figure 6.

Station	PNA	EP/NP	ENSO	PDO	NAO
46001	0.41	0.09	0.10	0.13	-0.49
46002	0.65	-0.31	-0.07	0.48	-0.45
46006	0.74	-0.25	-0.49	-0.15	-0.56
46035	0.48	-0.53	-0.64	-0.14	-0.49

Table 2. Correlation Coefficients (R^2) between Pacific Stations and Climate Indices

Menendez et al. (2008) state that the three most influential North-Eastern Pacific teleconnections are the PNA, EP/NP and ENSO indices. However, they also point out that these indices are not independent but between them represent a significant portion of inter-annual and inter-decadal climate change in this area.

The most convincing teleconnection is a positive relationship between Hmp-100 at all stations and the PNA index. The relationship is strongest for station 46006, shown in Figure 14, perhaps due to the proximity of this station to the mean North Pacific winter cyclone track.

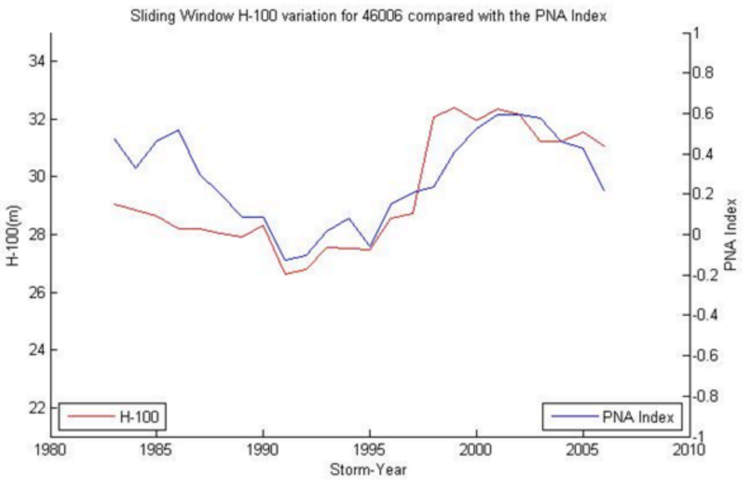

Figure 14. PNA Index plotted with wave extremes for station 46006

Relationships for the EP/NP and ENSO Nino 3.4 indices are less clear. The relationships at 46001 and 46002 are weak. However the relationships are stronger at 46006 and 46035 especially when seen plotted with the index reversed. A recent opinion is that the ENSO Nino 3.4 index is associated with a deepening of the Aleutian low and a strengthening of winter depressions (Menendez et al., 2008). Our results appear to contradict this hypothesis so further investigation is required. Weaker correlations with the ENSO Nino 3.4 index might be expected because the El Nino-Southern Oscillation is a global equatorial phenomenon whereas NP and PNA are specific to the region of interest. Correlations with the Pacific Decadal Oscillation (PDO) were considered but no prevailing trends could be found.

Although the NAO is an Atlantic phenomenon, the nature of teleconnections is that they can have effects outside their supposed area of influence. The NAO is the most dominant oscillation in the Northern hemisphere (Menendez, 2008), so a significant negative correlation illustrates the teleconnection from the North Atlantic to 100-year estimates of extreme waves in the North Pacific.

4 Conclusion

Summary of Wave Results

Station	Observed Hs-max (m)	H_{mp-100} (m)	$H_{mp-1000}$ (m)	$H_{mp-1000}$ / H_{mp-100}
46001	13.88	26.7	30.0	1.12
46002	13.5	28.2	32.0	1.14
Haltenbanken	13.97	31.3	36.3	1.16
46035	15.4	31.8	37.3	1.17
46006	16.32	31.9	37.3	1.17

4.1 Overall results

- The principal results from the Weibull fits are shown in the table above. Extreme waves on the open ocean are large! The 100-year most probable maximum wave heights are roughly 2x the largest observed Hs value.
- The most probable maximum wave height Hmp is a robust parameter for describing the severity of a storm with a single value, it contains input from both the significant wave height and storm duration.
- The forms of the extreme wave Hmp fits appear to be consistent between locations. The ratio of the 1000 to 100 year extreme wave height slowly increases as the severity of the environment increases from 1.12 for station 46001 to 1.17 for stations 46006 and 46035, and the North Atlantic Norwegian location also fits into this same pattern.
- In the North Pacific, stations 46006 (far offshore California) and 46035 (Bering Sea) have the most violent wave climates and there is substantial inter-annual variation of Hmp-100. In contrast, stations 46001 (Gulf of Alaska) and 46002 (offshore California-Oregon) each have a remarkably constant and less severe wave climate.

4.2 Extreme Waves and Climate Indices

North Atlantic offshore Norway and the NAO

- A very strong positive correlation was observed between the NAO and the extreme wave dataset based on a 5-year sliding window, allowing variation of the extreme wave climate to be estimated over almost 200 years.
- There appear to have been extremes of the wave climate before 1960 significantly more severe than any seen since.

North Pacific Indices

- The most convincing result is a positive correlation at all stations with the Pacific North American pattern. It is particularly strong at station 46006. El Nino has some influence but the Pacific Decadal Oscillation varies too slowly to be identified in the analysis. There are also medium strength negative correlations with the North Atlantic Oscillation at all stations in the North Pacific, showing the global reach of teleconnections.

Acknowledgement: The authors are grateful to Dr. Colin Grant of BP for access to the Haltenbanken dataset. The views expressed in this paper are solely those of the authors.

References

Allan, J., and P. Komar (2000), Are ocean wave heights increasing in the eastern North Pacific?, *Eos Trans. AGU*, 81, 561– 567.

Bacon, S., and D. J. T. Carter (1991), Wave climate changes in the North Atlantic and North Sea, Int. *J. Climatol*., 11, 545– 558.

Biondi, Franco; Gershunov, Alexander; Cayan, Daniel R. (2001), North Pacific Decadal Climate Variability since 1661, *Journal of Climate,* 14 (1), 5–10.

Bjerknes, J. (1966), A possible response of the atmospheric Hadley circulation to equatorial anomalies in ocean temperature, *Tellus*, 18, 820–829.

Carter, D. J. T., and L. Draper (1988), Has the North-east Atlantic become rougher? *Nature*, 332, 494.
Climate Prediction Center Internet Team, NOAA Climate Prediction Centre (CPC), 5/4/2009
Diaconis, P. and B. Efron (1983) Computer Intensive methods in statistics. *Scientific American*, May 1983, 96-108.
Hurrell J., G. Kushnir, G. Otterson, M. Visbeck (2003), *The North Atlantic Oscillation: Climatic and Environmental Impact (Geophysical Monograph)* (Hardcover), American Geophysical Union
Mantua, N. J., S. R. Hare, Y. Zhang, J. M. Wallace, and R. C. Francis (1997), A Pacific interdecadal climate oscillation with impacts on salmon production. *Bull. Amer. Meteor. Soc.,* 78, 1069–1079.
Menendez, M.,F. J. Mendez, I. J. Losada, and N. E. Graham (2008), Variability of extreme wave heights in the Northeast Pacific Ocean based on buoy measurements, *GRL*, 35, L22607, doi:10.1029/ 2008GL035394.
NDBC webmaster, NOAA National Data Buoy, Centre www.ndbc.noaa.gov, 5/4/2009
Osborn T.J. (2006), Recent Variations in the winter North Atlantic Oscillation, *Weather*, 61, 1-12.
Taylor, P.H. and J.Y.K. Goh (2000), Extrapolation of long term storm statistics: The POT method and data transformation, *19th Int. Conf. on Offshore Mechanics and Arctic Eng.,* Feb 14-17, 2000, OMAE00-6127
Tromans, P.S. and L. Vanderschuren (1995), Response based design conditions in the North Sea: application of a new method, *Proc. 27th Int. Conf. on Offshore Technology*, OTC7683.
Wallace, J. M., and D. S. Gutzler (1981), Teleconnections in the geopotential height field during the Northern Hemisphere winter, *Mon. Weather Rev.,* 109, 784– 812.
Woolf, D. K., P. G. Challenor, and P. D. Cotton (2002), Variability and predictability of the North Atlantic wave climate, *J. Geophys.Res*., 107(0)

Appendix - Climatic Phenomena

North Atlantic Oscillation (NAO) - data source: www.cru.uea.ac.uk
The NAO is a predominantly atmospheric mode measured by the normalized sea level pressure difference between Gibraltar and South-West Iceland (the centres of action).

Pacific/ North American (PNA) - data source: www.cpc.noaa.gov
The Pacific/ North American pattern (PNA) is one of the most prominent modes of low-frequency variability in the Northern Hemisphere extra-tropics (Hurrell et al, 2003). There are four centres of action, two in the North Pacific and two over North America. Fluctuations near the Aleutian Islands vary out of phase with those to the south forming a see-saw that pivots along the mean position of the Pacific sub-tropical jet stream.

East-Pacific North Pacific (EP/NP) - data source: www.cpc.noaa.gov
The EP/NP pattern has three centres of actions. The positive phase of this pattern features positive pressure anomalies located over Alaska and negative anomalies over the central North Pacific and eastern North America. Negative phases of the pattern are associated with circulation anomalies of opposite sign in these regions.

El-Nino Southern Oscillation (ENSO) - data source: www.cpc.noaa.gov
ENSO refers to the year-to-year variations in sea-surface temperatures, convective rainfall, surface air pressure, and atmospheric circulation across the equatorial Pacific Ocean. The Nino 3.4 index is a widely used area average measure of the eastern tropical Pacific SST (sea surface temperature). SST in the equatorial North Pacific alters winter circulation and storm activity over the North Pacific (Menendez et al., 2008, Bjerknes, 1966). Menendez et al. (2008) also report an expanded Aleutian Low during El Nino years and consequently rougher wave conditions in the eastern and central North Pacific

Pacific Decadal Oscillation (PDO)) - data source: jisao.washington.edu/pdo
The Pacific Decadal Oscillation (PDO) is a long-term fluctuation of the Pacific Ocean. The cool phase is characterised by a cool wedge of lower than normal sea-surface heights/ocean temperatures in the eastern equatorial Pacific and a warm horseshoe pattern of higher than normal sea-surface heights connecting the north, west and southern Pacific. In the warm phase the pattern reverses. There have only been two full PDO cycles in the past century so the cycles appear too slow to be visible within the shorter wave records analysed in this paper.